Biogeochemistry
https://doi.org/10.1007/s10533-019-00544-x

Historical soil drainage mediates the response of soil greenhouse gas emissions to intense precipitation events

Alexander Krichels · Evan H. DeLucia · Robert Sanford · Joanne Chee-Sanford · Wendy H. Yang

Received: 2 October 2018 / Accepted: 22 January 2019

Abstract Precipitation events are increasing in intensity in the Midwestern US due to climate change. This is resulting in flooding of poorly-drained upland soils, which can feed back on climate change by altering greenhouse gas (GHG) emissions, including nitrous oxide (N_2O) and carbon dioxide (CO_2). The objective of this study was to determine if soil drainage history affects the response of soil GHG emissions to rain events. To do this, we measured N_2O and CO_2 fluxes from poorly-drained (PD) and well-drained (WD) soils in an agricultural field in Urbana, Illinois before and after large rain events. We also performed a lab experiment to separate effects of soil drainage history from contemporary effects of ponding. Finally, we utilized stable isotope techniques to measure gross N_2O dynamics and to determine the contributions of nitrifiers and denitrifiers to net N_2O fluxes. We found that ponding of WD soils led to pulses of net N_2O efflux caused by stimulation of gross N_2O production by denitrifiers. In contrast, PD soils had high net N_2O effluxes only between large rain events, and gross N_2O production was inhibited following ponding. Soil CO_2 efflux was greater from PD soils under lab conditions, but autotrophic respiration obscured this trend in the field. Soil GHG emissions were a result of different contemporary ponding status as well as historical soil drainage, suggesting that historical soil redox regimes regulate soil GHG dynamics in response to precipitation. These soil drainage legacy effects are likely important in predicting soil GHG feedback effects on climate change.

Keywords Denitrification · Drainage · Nitrification · Nitrous oxide · Redox · Soil oxygen

Responsible Editor: Edith Bai.

Electronic supplementary material The online version of this article (https://doi.org/10.1007/s10533-019-00544-x) contains supplementary material, which is available to authorized users.

A. Krichels (✉) · E. H. DeLucia · W. H. Yang
Program in Ecology, Evolution, and Conservation Biology, University of Illinois, Urbana, IL 61801, USA
e-mail: krichel2@illinois.edu

E. H. DeLucia · W. H. Yang
Department of Plant Biology, University of Illinois, Urbana, IL 61801, USA

R. Sanford · W. H. Yang
Department of Geology, University of Illinois, Urbana, IL 61801, USA

J. Chee-Sanford
US Department of Agriculture—Agricultural Research Service, Urbana, IL 61801, USA

Introduction

The frequency and magnitude of intense precipitation events is increasing globally (USGCRP 2009; Min et al. 2011). In the Midwestern US, heavy rainfall has

Published online: 31 January 2019

led to higher frequency, duration, and spatial extent of ponding of upland mesic soils (Gleason 2008; Villarini et al. 2013). Changes in soil redox conditions associated with contemporary ponding can alter rates of biogeochemical processes that contribute to soil–atmosphere fluxes of greenhouse gases (GHGs), such as nitrous oxide (N_2O) and carbon dioxide (CO_2) which feedback on climate change. Depressions in the landscape that are more prone to ponding contribute disproportionately to ecosystem level GHG fluxes (Ambus and Christensen 1994; Ball et al. 1997; Li et al. 2018; Turner et al. 2016). However, as the spatial extent of ponding increases in the future, soil GHG dynamics in these newly ponded areas may not be similar to those in historically ponded areas. This can result from differences in soil chemistry, structure, microbial community composition, and other factors developed from long-term differences in soil moisture or drainage patterns (Averill et al. 2016; DeAngelis et al. 2010; Groffman and Tiedje 1991; Hawkes et al. 2017; Hawkes and Keitt 2015; Zeglin et al. 2013). Here, we differentiate soils based on soil drainage classification determined by the presence of ponding after large rain events. We define soil drainage legacy as differences in soil biotic and abiotic properties as a result of differences in historical soil drainage. The role of soil drainage legacy on the response of soil GHG dynamics to intense precipitation events has not been previously explored, yet it may be important in accurately predicting soil GHG feedback effects on climate change.

Water inundation effects on soil GHG dynamics in upland ecosystems that experience episodic ponding differ from those in perennially flooded ecosystems, such as wetlands and peatlands. In flooded ecosystems, soil–atmosphere GHG fluxes are dominated by methane (CH_4) due to the depletion of terminal electron acceptors (TEAs) higher on the redox ladder, such as oxygen (O_2) and nitrate (NO_3^-), which are needed for CO_2 and N_2O production (Estop-Aragonés et al. 2013; Knowles 1982). In soils that experience fluctuating redox conditions, these TEAs are replenished during periods when soils are unsaturated and oxic. When the soils inundate, the reduction of these replenished TEAs can then be coupled with organic C oxidation to anaerobically produce CO_2. This phenomenon can be important at the ecosystem level, with the reduction of iron (Fe) accounting for up to 40% of CO_2 emissions in upland soils that experience fluctuating redox conditions (Dubinsky et al. 2010). Soil NO_3^- pools are replenished by nitrification during oxic periods, and can drive N_2O production from denitrification, a multi-step anaerobic process which reduces NO_3^- to N_2O and then reduces N_2O to dinitrogen (N_2) when NO_3^- is limiting relative to electron donors such as C (Firestone et al. 1980). After rain events, topographic depressions can act as transient hot spots of soil N_2O emissions due to increased soil moisture (Turner et al. 2008, 2016; Yanai et al. 1965). Furthermore, NO_3^- and dissolved organic matter can accumulate in topographically depressed areas, possibly as a result of lateral movement of water, further fueling these hotspots of denitrification (Turner et al. 2008, 2016; Yanai et al. 1965). Although depressions may not perpetually act as N_2O hot spots, short-lived high N_2O emissions can act as hot moments that have been shown to account for up to 51% of cumulative annual N_2O emissions (Kroon et al. 2007; Molodovskaya et al. 2012; Parkin and Kaspar 2006; Saha et al. 2017). Understanding the controls over GHG emissions from different soil drainage classes that become transient hot spots under different conditions could, therefore, be important to accurately predict how soil GHG fluxes will respond to rainfall intensification associated with climate change.

Changes in soil chemistry, physical structure, and microbial community composition caused by historical soil drainage may control the response of biogeochemical processes to contemporary environmental conditions, such as ponding. Short-term legacy effects resulting from different precipitation and moisture regimes on the scale of days to months have been shown to affect soil CO_2 emissions (Groffman and Tiedje 1988; Evans and Wallenstein 2012; Averill et al. 2016). Soil moisture hysteresis can also affect soil N_2O fluxes (Groffman and Tiedje 1988; Banerjee et al. 2016). Over the long term, repeated ponding and soil redox fluctuations can affect organic C availability for heterotrophic microbial activity by slowing plant growth (Grable and Siemer 1968; Kanwar et al. 1988), facilitating the release of labile C from organo-mineral complexes (De-Campos et al. 2012; Huang and Hall 2017; Thompson et al. 2011), and breaking down soil aggregates (Adu and Oades 1978; De-Campos et al. 2009). The breakdown of soil aggregates by ponding can also alter the distribution of O_2 in soil and destroy

hypoxic microsites that act as hotspots of N_2O production via denitrification after soil drainage (Algayer et al. 2014; Sey et al. 2008). Fluctuating soil redox in depressions in surface soils can increase the bioavailability of Fe oxides over time by changing their mineralogy towards increasingly poorly crystalline forms that are more reactive than crystalline minerals (Ginn et al. 2017; Thompson et al. 2011). Additionally, soil microbial communities can adapt to dynamic redox regimes (Banerjee et al. 2016; DeAngelis et al. 2010; Evans and Wallenstein 2012, 2014; Palta et al. 2016; Peralta et al. 2013; Pett-Ridge et al. 2006; Zeglin et al. 2013). Any of these factors or combination of these factors may control soil GHG emissions depending on historical soil drainage. Lasting changes to soil biotic and abiotic properties can occur over the course of a single growing season (Pett-Ridge et al. 2006; De-Campos et al. 2009, 2012; Banerjee et al. 2016; Ginn et al. 2017) but can also take many years to develop (Thompson et al. 2011; Evans and Wallenstein 2012, 2014; Zeglin et al. 2013; Averill et al. 2016).

The goal of this study was to determine if historical soil drainage affects the response of CO_2 and N_2O emissions from upland soils to intense precipitation events. To test our hypothesis that CO_2 and N_2O dynamics would differ between soils with different historical drainage patterns, we measured in situ CO_2 and N_2O fluxes from poorly-drained and well-drained areas in an active agricultural field prior to and following large rain events. Soil drainage classifications were determined based on visual observations of ponding only in areas classified as poorly-drained in the days following large rain events (> 30 mm over 24 h). To separate the effects of contemporary conditions from soil drainage legacy effects, we performed a laboratory experiment in which soils from both drainage classes were subjected to the same flooding and drainage treatments. We also used stable isotope pool dilution techniques to measure gross N_2O production and consumption in the field, and stable isotope tracers to determine the dominant process responsible for N_2O production in the lab.

Methods

Study site

The study was conducted in an agricultural field located at the University of Illinois Crop Sciences Research and Education Center in Urbana, Illinois (40°4′26.42″N, 88°14′19.63″W). For over the past 50 years, the field has been primarily rain-fed and is annually planted in maize in odd years and soybeans in even years, including in 2014 and 2015. Mean annual temperature in Urbana is 10.9 °C, and mean annual precipitation is 1045 mm (Illinois Climate Network 2017). Precipitation data for the time period of this study were measured 0.5 km away from the study site (Illinois Climate Network 2017). During the period of 1989–2012, the daily average air temperature for the growing season (June–September) ranged between 22 and 24 °C; the monthly average rainfall ranged between 70 and 110 mm for this period (Illinois Climate Network 2017).

The study field extends approximately 80 m from north to south along a drainage gradient that causes varying frequency and duration of ponding in response to rain. This ponding occurs despite underlying tile drainage typical of the Midwest, US. Soils in the northern end of the field are classified as somewhat poorly-drained silt loams from the Flanagan soil series, while soils in the southern end are classified as poorly-drained silty clay loams from the Drummer soil series. These geographically associated soil series occur along a slope profile forming a drainage sequence with the Drummer soil in depressed areas; in other words, the characteristics that distinguish the two soil series are caused by the differing historical drainage patterns along the slope profile. We established two circular sampling areas (10 m diameter) separated by 60 m along this soil drainage gradient and for simplicity in terminology hereafter refer to the drainage class on the north end as well-drained (WD) and on the south end as poorly-drained (PD). The PD soils exhibit ponding when over 30 mm of precipitation fall over 24 h whereas the WD soils never experience ponding. Both the PD and WD soils are under the same management practices.

Quasi-continuous in situ measurements

To characterize how soil redox in the two drainage classes responded to precipitation, we measured quasi-

continuous in situ bulk soil O_2 concentrations and volumetric water content as proxies for soil redox. Soil O_2 data were collected from 10, 20, and 30 cm depth at one location in each drainage class beginning 10 May 2015 using Apogee SO-110 oxygen sensors fitted with AO-001 diffusion heads (Apogee Instruments, Logan, UT). Sensor voltage was measured every minute, and 30-min averages were recorded on a CR-100 datalogger (Campbell Scientific, Logan, UT). We converted voltage measurements to relative percent O_2 using a unique calibration factor for each probe determined prior to field deployment. The probes were calibrated based on mV measurements at 0% O_2 (dinitrogen gas) and 20.95% O_2 (ambient air) in sealed jars containing water to create a humid environment that mimicked mesic soil conditions. We used an empirical function provided in the Apogee SO-110 owner's manual to correct soil O_2 concentrations for temperature in the diffusion head as measured by the SO-110 sensor and atmospheric pressure measured at a nearby weather station (Illinois Climate Network 2017). Soil moisture was measured quasi-continuously using Decagon 5TM probes with EM50 data loggers at 10 cm and 30 cm depth from the PD class from April 2015 through September 2015 (Decagon, Pullman, WA); data are absent from the WD drainage class due to a non-operational datalogger.

Field measurements of net GHG fluxes

We measured in situ net GHG fluxes in the WD and PD classes on 11 dates during June–July 2014, a period when we expected large rain events to occur. We aimed to quantify fluxes before and after large rain events (> 30 mm) that could cause ponding and were successful in doing so for one event in late June. On each sampling date, we randomly placed six 26 cm diameter, 10 cm tall polyvinylchloride collars in each drainage class, inserting each collar approximately 3 cm into the soil surface. After a 30 min equilibration period, a vented acrylonitrile–butadiene–styrene plastic chamber top with a rubber septum port was placed on each collar (Matson et al. 1990). Gas samples were collected at 0, 5, 15, 30, and 45 min after the chambers were sealed; they were stored in 10 mL pre-evacuated glass vials sealed with thick rubber septa (Geo-Microbial Technologies, Inc., Ochelata, OK) and aluminum crimps (Wheaton Industries, Inc., Millville, NJ). All gas samples were analyzed on a Shimadzu GC 2014 gas chromatograph (GC) equipped with an electron capture detector (ECD), flame ionization detector, and thermal conductivity detector to measure concentrations of N_2O, CH_4, and CO_2, respectively. We determined net trace gas fluxes from the change in gas concentration over time using an iterative model that fits an exponential curve to the data (Matthias et al. 1978). Fluxes were considered to be zero when there was no significant relationship between gas concentration and time ($p > 0.05$). There were no significant net CH_4 fluxes measured in this study.

Soil physical and chemical properties were also measured from each gas sampling location to provide insight into possible mechanisms driving observed patterns in soil GHG fluxes. After the last gas sample was collected from a chamber, we measured the chamber temperature and the soil temperature at 10 cm depth in the chamber footprint using an Acorn Temp 5 meter (Oakton Instruments, Vernon Hills, IL). A 0–10 cm depth soil sample was collected from each chamber footprint and transported at ambient temperature to the laboratory for same day processing. A subsample of each homogenized soil sample was shaken in 2 M KCl for 1 h, and another was shaken in 0.5 N HCl for 24 h to extract inorganic N and acid-extractable Fe, respectively. KCl extracts were analyzed colorimetrically for NH_4^+ and NO_3^- on a Lachat Quick Chem flow injection analyzer (Lachat Instruments, Milwaukee, WI, USA). HCl extracts were analyzed for total Fe and Fe(II) concentrations using a modified ferrozine method (Liptzin and Silver 2009) on a Genesys 5 spectrophotometer (Thermo Scientific Spectronic, Waltham, MA). We measured gravimetric soil moisture by oven-drying a soil sample at 105 °C for at least 48 h. As part of a separate study, we collected three 0–10 cm cores from each drainage class with a 5 cm diameter core (AMS, Inc., American Falls, ID) to measure soil pH and bulk density (Suriyavirun et al. 2019).

Field measurements of gross N_2O fluxes

To determine how gross N_2O production and consumption may have contributed to the patterns in in situ net N_2O fluxes we observed in 2014, we performed field measurements of gross N_2O fluxes following two large rain events from June to July 2015. We employed the $^{15}N_2O$ pool dilution technique

(Yang et al. 2011) with the same two-piece static flux chambers used for the net trace gas flux measurements. We volumetrically mixed 99% SF_6 (Matheson Tri Gas, Inc., Waverly, TN), 99% N_2O at 98 atom% ^{15}N enrichment (Isotech, Richmond, CA, USA), and ultra-high purity helium (Airgas, Radnor, PA) in gas sample bags (Restek Corporation, Bellefonte, PA) to create a spiking gas consisting of 7.7 ppm SF_6 and 13.1 ppm N_2O at 98% atom ^{15}N enrichment. We added 10 mL spiking gas to the chamber headspace immediately after the chamber top was placed on the collar, with the goal of increasing chamber headspace gas concentrations by 25 ppb N_2O and 10 ppb SF_6, achieving 5 atom% ^{15}N enrichment of the chamber headspace N_2O pool. Gas samples (90 mL) were collected 0, 5, 15, 30, and 45 min after spiking gas injection and were stored in pre-evacuated 60 mL glass vials sealed with Teflon-coated rubber septa (Macherey-Negal, Inc., Bethlehem, PA) and aluminum crimps (Wheaton Industries, Inc., Millville, NJ).

All gas samples were analyzed for trace gas concentrations and ^{15}N isotopic composition of N_2O in order to calculate gross rates of N_2O production and consumption. A 5 mL aliquot was removed from each gas sample vial for determination of N_2O, SF_6, CH_4, and CO_2 concentrations on the GC. For this experiment, the GC was equipped with a 4 m × 1 mm Hayesep Q column to allow adequate separation between N_2O and SF_6 on the ECD. The remaining gas in each sample vial was analyzed for ^{15}N isotopic composition of N_2O using an IsoPrime 100 isotope ratio mass spectrometer (IRMS) interfaced to a trace gas preconcentration unit (Isoprime Ltd., Cheadle Hulme, UK) and a GX-271 autosampler (Gilson, Inc., Middleton, WI). To calculate rates of gross N_2O production and consumption we used the pool dilution model described by Yang et al. (2011) and von Fischer and Hedin (2007). The iterative model solves for N_2O production based on the dilution of the isotopically enriched chamber headspace pool of N_2O by natural abundance N_2O. Gross consumption rates were estimated using the empirical loss of ^{15}N–N_2O, using SF_6 as a tracer to account for physical loss. We assumed that the isotopic composition of produced N_2O was 0.3431 atom% ^{15}N and the fractionation factor associated with N_2O reduction to N_2 was 0.9924 (Yang et al. 2011). N_2O yield was calculated as the difference between gross N_2O production and consumption divided by gross N_2O production.

N_2O source lab experiment

In September 2015, we collected 24 intact soil cores (0–10 cm depth) from each of the WD and PD classes for a laboratory ^{15}N tracer experiment to estimate the relative importance of nitrifiers and denitrifiers in producing N_2O. We collected the cores from relatively dry soils to reduce the potential for soil compaction. We used a 2.5 cm diameter corer (AMS, Inc., American Falls, ID) fitted with removable plastic sleeves to collect the intact cores. We discarded cores that were clearly compacted during collection; the bulk density of the cores used in the experiment were comparable to that of cores collected using a 5 cm diameter corer (1.03 ± 0.10 and 1.09 ± 0.10 g dry soil cm^{-3} using the 2.5 cm corer in PD and WD soils, respectively compared to 1.05 ± 0.06 and 0.97 ± 0.02 g dry soil cm^{-3} using the 5 cm corer for PD and WD soils, respectively). We removed sleeved soil cores from the corer and capped them at both ends prior to transport to the laboratory at ambient temperature. Soil cores were incubated upright, with the upper cap removed, in a dark growth chamber (model PGR15, Conviron, Winnipeg, Canada) set to mimic mean typical summertime diurnal temperature fluctuations (12 h at 20 °C and 12 h at 30 °C) determined from quasi-continuous in situ surface soil (5 cm depth) temperature measurements at the site in 2011–2013 (Sanford unpublished data). Soil evaporation during the 2-day preincubation was minimized by placing a tub of water in the growth chamber to increase humidity and by loosely covering the cores with aluminum foil.

We imposed a flooding treatment and a drainage treatment to determine if N_2O production pathways differed between PD and WD soils under different moisture conditions. After 2 days of the preincubation described above, we flooded all 24 of the cores from each drainage class with rainwater. Half of the cores (n = 12 for each drainage class) were drained after 2 days (referred to as the Drained treatment), and half of the cores remained flooded for the full 5-day incubation period (referred to as the Flooded treatment). Net fluxes of N_2O, CO_2, and CH_4 were measured prior to flooding the cores (day 1) and on days 2 through 4 of the treatment incubations. Each day the same two intact soil cores from a given treatment were placed together in a sealed jar for net trace gas flux measurements to yield six replicate

measurements per treatment. Real-time trace gas concentrations in the jar headspace were measured over 8 min using a cavity ring down spectrometer (CRDS; Model G2508, Picarro, Santa Clara, CA); trace gas fluxes were estimated from the linear change in concentrations, excluding the first minute of data when the gases were mixing between the jar, CRDS internal headspace, and the tubing connecting the jar to the Picarro (with a total of 174 mL volume sample loop). Fluxes were considered significant if the change in gas concentration exceeded three times the reported 5-min detection limit (0.015 ppm for N_2O and 0.6 ppm for CO_2, Model G2508, Picarro, Santa Clara, CA).

To estimate N_2O production from nitrifiers and denitrifiers, we used short-term laboratory incubations with either ^{15}N-labeled NH_4^+ or ^{15}N-labeled NO_3^- (n = 6 for each treatment). The production of $^{15}N_2O$ from soils receiving $^{15}NH_4^+$ represents nitrifier nitrification and nitrifier denitrification as N_2O source processes (van Groenigen et al. 2015) and from soils receiving $^{15}NO_3^-$ represents heterotrophic denitrification. We did not account for abiotic processes, which can be important sources of N_2O in arid and semi-arid systems (Wang et al. 2017) but are likely less important in our mesic study site. On the final day of the treatment incubation (day 5), the soil samples were extruded from their cores and composited in Ziploc bags in the pairs that had been used for the CRDS trace gas flux measurements. We did this to ensure homogenous ^{15}N enrichment in the soil. The homogenized soil samples were subsampled to measure gravimetric moisture and for 2 M KCl extraction to determine initial background NH_4^+ and NO_3^- concentrations. We split the remaining soil into two subsamples for ^{15}N label addition: 1 mL of 99 atom% ^{15}N enrichment NH_4Cl (Cambridge Isotope Laboratories, Inc., Andover, MA) at a solution concentration of 6.38 μg N mL^{-1} was added to one subsample, and 1 mL of 99 atom% ^{15}N enrichment KNO_3 (Cambridge Isotope Laboratories, Inc., Andover, MA) at a solution concentration of 5.83 μg N mL^{-1} was added to the other. The initial ^{15}N enrichment of the NH_4^+ pool averaged 15.2 atom% and ranged 3.6–33.2 atom%. The initial ^{15}N enrichment for the NO_3^- pool averaged 17.8 atom% and ranged 4.1–36.9 atom%. After 15 min, 25 g of each soil sample was extracted in 100 mL of 2 M KCl. The remaining soil was sealed in a 250 mL canning jar with a lid fitted with a rubber septum. After 4 h, a 90 mL gas sample was collected from the jar, and then the soil in the jar was extracted for NH_4^+ and NO_3^- in 2 M KCl. Soil NH_4^+ and NO_3^- in the KCl extracts were prepared for ^{15}N isotope analysis by acid-trap diffusion (Herman et al. 1995) and analyzed for ^{15}N isotopic composition on an IsoPrime 100 IRMS interfaced to a Vario Micro Cube elemental analyzer (Isoprime Ltd., Cheadle Hulme, UK; Elementar, Hanau, Germany). The gas samples were analyzed for trace gas concentrations on a GC and for ^{15}N–N_2O on an IRMS as described above. Net CO_2 and N_2O emissions were calculated by the change in concentration over the course of the incubation. We calculated a minimal detectible flux based on the standard deviation of three standard gas samples (1001 ppm CO_2 and 1.08 ppm N_2O) run on the GC. The calculated detection limit for N_2O was 0.007 ppm h^{-1} for CO_2 was 5.6 ppm h^{-1}. We estimated fluxes below this detection limit as zero. We estimated nitrifier-derived net N_2O fluxes based on $^{15}N_2O$ produced from soils amended with $^{15}NH_4^+$ scaled by the mean ^{15}N enrichment of the NH_4^+ pool measured at the 15 min and final time points. Denitrifier-derived net N_2O fluxes were similarly estimated using the samples amended with $^{15}NO_3^-$. The sum of the nitrifier- and denitrifier-derived N_2O fluxes estimated in this way exceeded the net N_2O flux determined simply from the change in N_2O concentration (i.e., the net flux of $^{14}N_2O + {}^{15}N_2O$) due to N_2O reduction to N_2 via denitrification during the soil incubations. This does not affect our aim to determine the relative contribution of nitrifiers and denitrifiers to N_2O. Therefore, we calculated the proportional contribution of each process to the sum of nitrifiers- and denitrifiers-derived N_2O fluxes and then proportionally adjusted the N_2O flux estimates for each process so that their sum equaled the net N_2O flux.

Statistical analysis

We used R version 3.5.1 (R Core Team 2014) to perform statistical analyses and Microsoft Excel version 14.7.7 (Microsoft Corporation, Redmond, WA, USA) to run the iterative pool dilution model. Differences in soil physical and chemical variables measured in the field from WD and PD soils were assessed using two-tailed Student's *t* test. Statistical

significance was determined at $p < 0.05$. We used two-way analysis of variance (ANOVA) with drainage class and date as factors to compare field fluxes and soil properties before and after one large rain event spanning June 23rd and 24th 2014. This was done using the anova function in the car package in R (Fox and Weisberg 2011). Type III sums of squares were used to test for the presence of an interaction. If no interaction was detected, then type II sums of squares were used. When needed, data were either square root transformed or log-transformed to meet the assumptions of normality. A small constant of one was added prior to transformation when values below one were present. We used linear mixed effects models with drainage class and day of experiment as the two fixed factors, and soil core ID as the random factor to assess differences in net CO_2 and N_2O emissions from flooded cores during days 2 through 4 of the N_2O source lab experiment. This was done using the lme function from the nlme package (Pinheiro et al. 2017). We tested the significance of the fixed factors in this model using a likelihood ratio test performed using the anova function in car (Fox and Weisberg 2011). We used two-way ANOVA with treatment and drainage class as the factors to compare nitrification and denitrification derived N_2O fluxes from the N_2O source lab experiment. We conducted multiple pairwise comparisons corrected using Tukey's HSD to compare means across all factors for both the field and lab measurements. This was done using the lsmeans package (Lenth 2016).

Results

Soil properties

Soil O_2 dynamics differed between the PD and WD classes from May 2015 through August 2015 (Fig. 1). During this time, the PD soils consistently had lower soil O_2 concentrations at 10 cm depth compared to the WD soils. After large rain events (i.e., over 30 mm in 24 h), 10 cm depth soil O_2 concentration in the PD class fell to as low as 0% and took up to a week to rebound to pre-rain levels (Fig. 1a, b). In contrast, soil O_2 in the WD class never dropped below 10% at 10 cm depth. Soil O_2 decreased with depth in both classes but was generally lower in the PD class across both depths (Fig. 1b, c). Volumetric soil moisture at 10 cm depth in the PD drainage class was close to 20% under dry conditions, and increased to around 35% in response to rain events (Fig. 1a, d). In general, 10 cm depth O_2 concentrations from PD soils began to decrease when soil moisture increased above approximately 30%.

Despite their proximity and similar management, soils from the two drainage classes had different chemical properties (Table 1). Soil from the PD class had higher concentrations of total organic C (TOC, $p < 0.01$) and total N ($p = 0.05$) compared to soils from the WD class. Soils from the PD class also had higher pH compared to soils from the WD class, averaging 5.85 ± 0.06 compared to 5.35 ± 0.07, respectively ($p < 0.01$). Soil bulk density was not significantly different between the two drainage classes, averaging 1.01 ± 0.05 g dry soil cm^{-3}.

Biogeochemical responses to rain events

Large rain events had strong and opposing effects on net N_2O fluxes between the two drainage classes (Fig. 2a, b), suppressing emissions in the PD class and stimulating them in the WD class ($F_{1,20} = 20.1$, $p < 0.001$). In response to a 64 mm rain event spanning June 23 and 24, 2014, N_2O emissions from the WD class increased from 3.0 ± 0.12 to 26 ± 12 ng N cm^{-2} h^{-1} ($p < 0.05$), whereas N_2O emissions from the PD class decreased from 15 ± 3.3 to 4.6 ± 2.0 ng N cm^{-2} h^{-1} ($p < 0.05$). This same pattern occurred in response to other rain events for which over 30 mm of precipitation fell within 24 h during June–July 2014 (Fig. 2a, b). There was no significant effect of sampling day on soil NH_4^+ concentrations ($F_{1,20} = 0.22$, $p = 0.6$), but there was a significant effect of drainage class ($F_{1,20} = 4.4$, $p < 0.05$), with PD soils having higher NH_4^+ concentrations (Fig. 2d). Soil NO_3^- concentrations decreased in response to the rain event ($F_{1,20} = 7.4$, $p = 0.01$), but this response did not differ between the two drainage classes ($F_{1,20} = 2.8$, $p = 0.1$) (Fig. 2e). HCl-extractable Fe(II) concentrations, used here as a biogeochemically relevant indicator of soil redox, were consistently higher for PD than WD soils ($F_{1,20} = 9.4$, $p < 0.01$) and did not change in response to the rain event ($F_{1,20} = 0.49$, $p = 0.49$) (Fig. 2f).

Field measurements of gross N_2O production and consumption rates during June–July 2015 elucidated

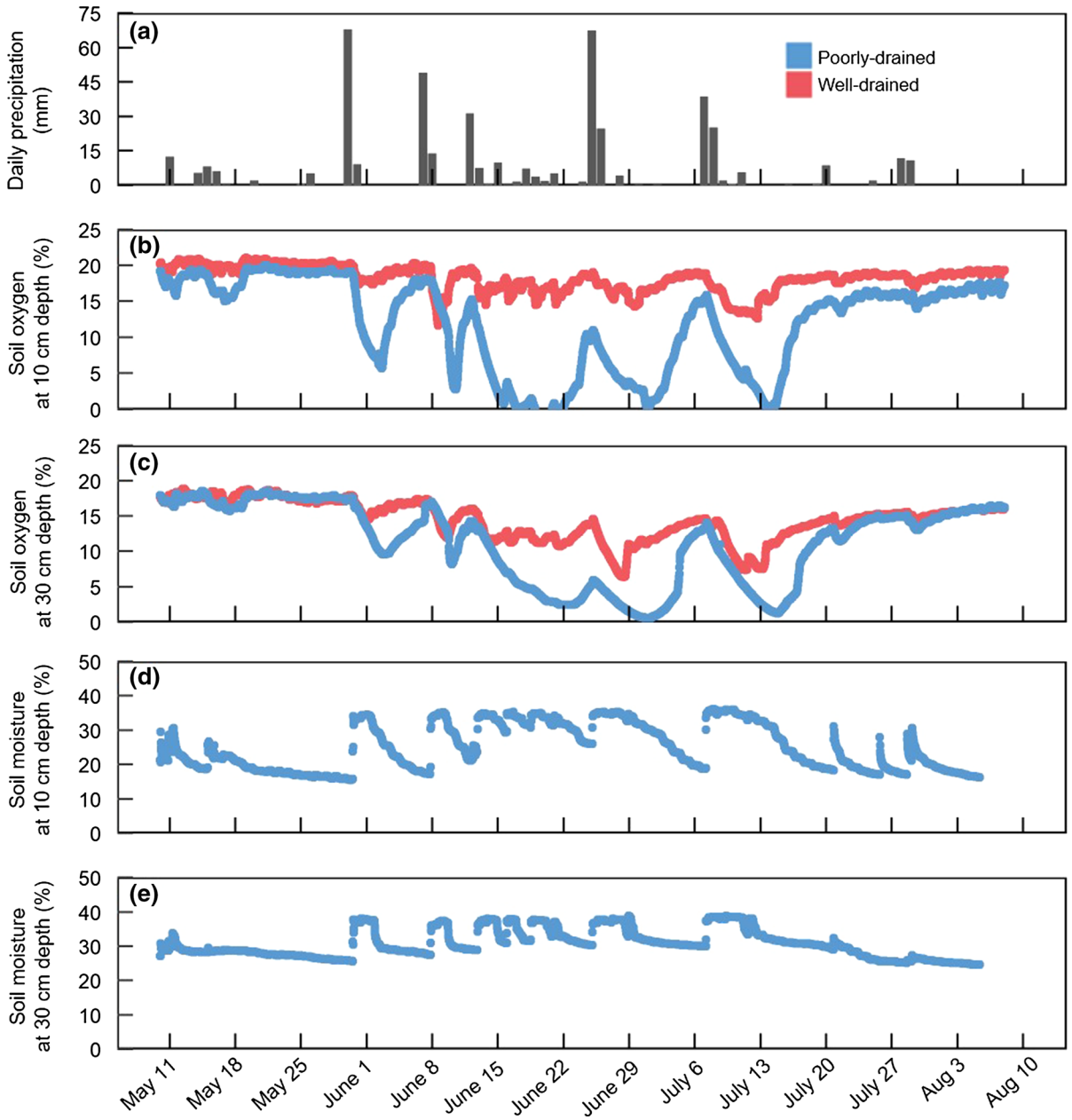

Fig. 1 Daily precipitation (**a**), bulk soil O_2 concentration at 10 cm depth (**b**) and 30 cm depth (**c**), volumetric soil moisture at 10 cm depth (**d**) and 30 cm depth (**e**) by drainage class. Data were collected from May through August 2015. Missing soil moisture data for the well-drained class was due to datalogger failure

the contribution of these two processes to net N_2O fluxes (Fig. 3). There was a significant drainage class by day interaction effect on N_2O yield ($F_{3,39} = 3.0$, $p < 0.05$), defined as net N_2O production divided by gross N_2O production (Table 2). The N_2O yield remained consistent in the WD class over the four sampling days in 2015, averaging 0.48 ± 0.08. In the PD class, the N_2O yield was lower on 27 June and 9 July compared to 11 July and 15 July (Table 2). Large rain events occurred within 48 h before sampling on 27 June and 9 July (Fig. 3a). This increase in N_2O yield was a result of a greater increase in gross N_2O production relative to gross N_2O consumption as soils dried on 11 July and 15 July, leading to a higher

Table 1 Soil chemical and physical properties by drainage class (mean ± standard error)

	n	t	p	Poorly-drained	Well-drained
Total organic C (%)	12	3.7	< 0.01	2.37 ± 0.05	2.16 ± 0.02
Total N (%)	12	2.1	0.05	0.182 ± 0.003	0.176 ± 0.001
pH	3	5.4	< 0.01	5.85 ± 0.06	5.35 ± 0.07
Bulk density (g cm^{-3})	3	1.4	0.30	1.05 ± 0.06	0.97 ± 0.02

A Student's t-test was performed to compare each soil chemical and physical property between the two drainage classes. Sample size (n), t-value (t), and p-value (p) from the Student's t-test are reported

proportion of produced N_2O being released to the atmosphere. Overall, net N_2O fluxes were inhibited in PD soils and were stimulated in WD soils following large rain events (Fig. 3b). This is the same pattern observed in 2014 (Fig. 2b) and appeared to be driven by suppressed gross N_2O production in PD soils following large rain events (Fig. 3c). Soil NO_3^- concentrations were greater in the WD class on 27 June, and were similar on all other sampling dates (Fig. 3e). Soil NH_4^+ concentrations were greater in the PD class compared to the WD class on 27 June, 9 July, and 11 July, and did not differ between drainage classes on 15 July (Fig. 3f).

Large rain events also differentially affected CO_2 fluxes in the two drainage classes ($F_{1,20} = 23.8$, $p < 0.001$) (Fig. 2c). On 23 June 2014, before the rain event, CO_2 fluxes averaged 25.9 ± 3.13 μg C cm^{-2} h^{-1} from PD soils compared to 16.2 ± 0.88 μg C cm^{-2} h^{-1} in WD soils. Afterwards, CO_2 fluxes decreased in the ponded PD soils ($p < 0.01$) whereas they did not change significantly in the WD soils, which did not have standing water. After this rain event, CO_2 fluxes were lower in the PD class (2.33 ± 0.56 μg C cm^{-2} h^{-1}) compared to the WD class (20.7 ± 4.70 μg C cm^{-2} h^{-1}; $p < 0.01$). Large rain events also inhibited CO_2 efflux from PD soils after large rain events on 30 June 2014 (Fig. 2c), as well 26 June and 7 July 2015 (Fig. 3g).

N_2O source laboratory experiment

One day of flooding stimulated net N_2O fluxes from both PD and WD classes (Fig. 4a). Fluxes were not detectable before the cores were flooded (day 1) and returned to non-detectable levels in the PD soil cores on day 3, after 2 days of flooding. During days 2 through 4, net N_2O fluxes were higher in the flooded WD soils compared to the flooded PD soils [$X^2(1) = 26.0$, $p < 0.001$, Fig. 4a]. There was also a significant day effect that was driven by lower N_2O efflux from the WD soils on day 4 [$X^2(2) = 8.7$, $p = 0.01$]. There was a marginally significant interaction effect of drainage class and day on net N_2O efflux ($F_{2,30} = 5.5$, $p = 0.06$).

There was a significant interaction effect on denitrifier-derived N_2O fluxes ($F_{1,16} = 5.9$, $p < 0.05$), with higher fluxes under the flooded treatment in the WD class compared to all other soils (Fig. 5a). Denitrifier-derived N_2O fluxes accounted for over 72% of the total net N_2O flux for all treatments across both drainage classes. The flooded treatment exhibited higher nitrifier-derived net N_2O fluxes than the drained treatment ($F_{1,18} = 9.8$, $p < 0.01$, Fig. 5b); there was no significant drainage class or interaction effect on these fluxes ($F_{1,18} = 0.85$, $p = 0.4$, $F_{1,18} = 0.84$, $p = 0.4$, respectively). There was a significant treatment effect on total net N_2O flux ($F_{1,43} = 12.27$, $p < 0.01$), and a marginally significant drainage class and interaction effects ($F_{1,43} = 3.8$, $p = 0.06$; $F_{1,43} = 3.8$, $p = 0.06$ respectively). Total net N_2O flux from the WD class under the flooded treatment was higher compared to all other drainage class and treatment combinations ($p < 0.05$).

Soil CO_2 fluxes were suppressed from all soils the day after flooding, but the fluxes rebounded during the experimental treatment incubation (Figs. 4b, 5d). During days 2 through 4 of the experiment, soil CO_2 fluxes in the flooded treatment were higher from the PD class compared to WD class [$X^2(1) = 11.0$, $p < 0.001$, Fig. 4b]. Additionally, CO_2 fluxes increased each day during this time [$X^2(2) = 10.9$, $p < 0.01$]. We also measured CO_2 efflux from soils during the N_2O source experiment (Fig. 5d). During this experiment, soil CO_2 fluxes were higher from the

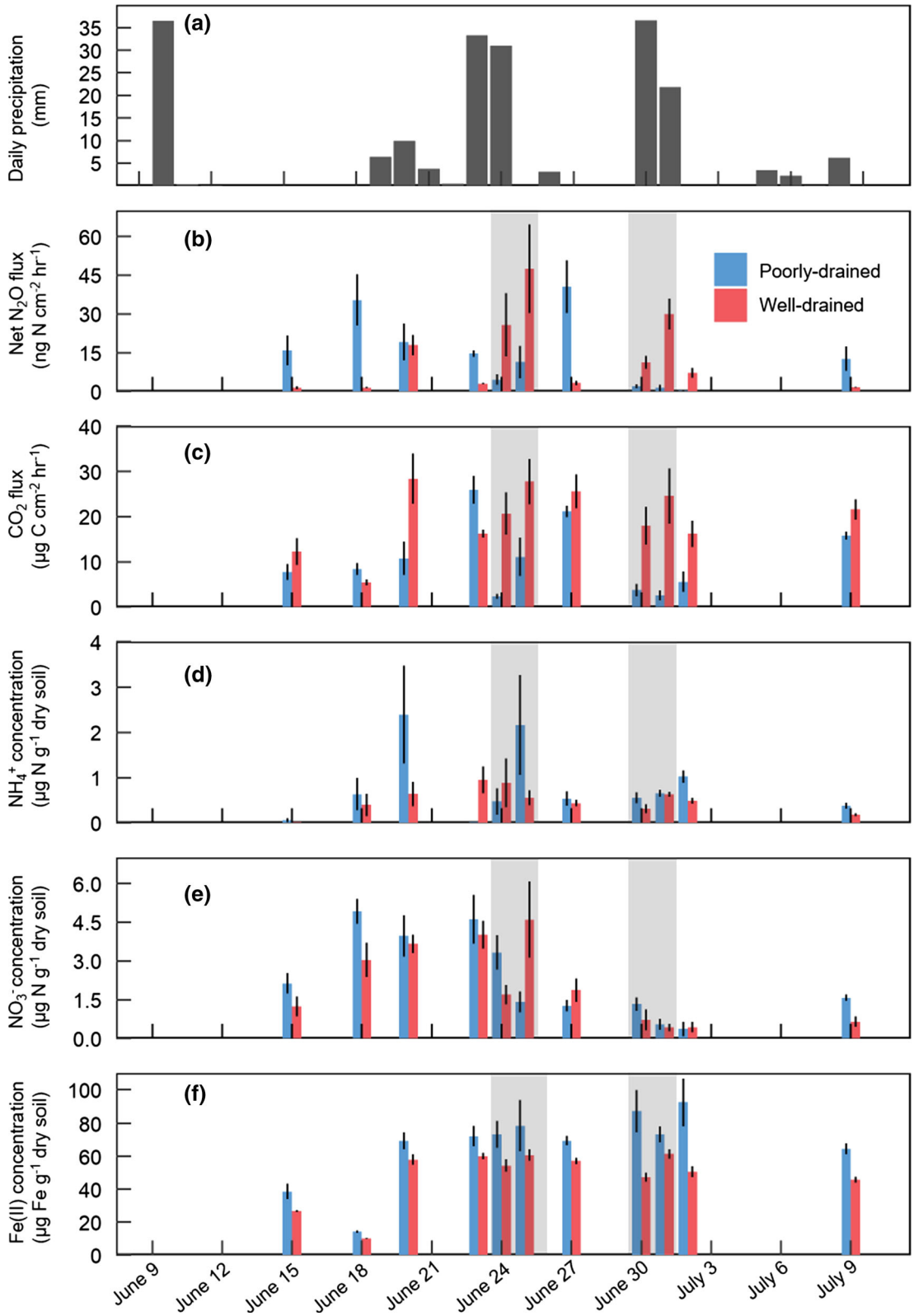
(a)
Daily precipitation (mm)
35
30
25
20
15
10
5
(b)
Net N_2O flux (ng N cm^{-2} hr^{-1})
60
45
30
15
0
Poorly-drained
Well-drained
(c)
CO_2 flux (µg C cm^{-2} hr^{-1})
40
30
20
10
0
(d)
NH_4^+ concentration (µg N g^{-1} dry soil)
4
3
2
1
0
(e)
NO_3^- concentration (µg N g^{-1} dry soil)
6.0
4.5
3.0
1.5
0.0
(f)
Fe(II) concentration (µg Fe g^{-1} dry soil)
100
80
60
40
20
0
June 9
June 12
June 15
June 18
June 21
June 24
June 27
June 30
July 3
July 6
July 9

◀**Fig. 2** Daily precipitation (**a**), net N_2O flux (**b**), CO_2 flux (**c**), and soil concentrations of NH_4^+ (**d**), NO_3^- (**e**) and Fe(II) (**f**) measured on 11 days during summer 2014. Error bars represent one standard error (n = 6). Shaded areas represent sampling days where over 30 mm of rain had fallen in the past 48 h

PD class compared to the WD class ($F_{1,44} = 11.6$, $p < 0.01$); overall, fluxes were higher in the flooded treatment compared to the drained treatment ($F_{1,44} = 17.2$, $p < 0.001$).

Soil NH_4^+ concentrations were higher in the flooded treatment than the drained treatment ($F_{1,20} = 19.7$, $p < 0.001$) but did not differ significantly between the two drainage classes ($F_{1,20} = 1.2$, $p = 0.3$, Fig. S1a). Nitrate concentrations immediately before the ^{15}N tracer addition were higher in the drained treatment than the flooded treatment ($F_{1,20} = 17.3$, $p < 0.001$) and were marginally higher in the WD class than the PD class ($F_{1,20} = 3.3$, $p = 0.08$) (Fig. S1b). Soil moisture was higher in the flooded treatment compared to the drained treatment ($F_{1,20} = 4.8$, $p < 0.05$, Fig. S1c). Before the soil cores were flooded, soil moisture did not differ between the two drainage classes, averaging 0.21 ± 0.01 g H_2O g^{-1} and 0.22 ± 0.01 g H_2O g^{-1} in the PD and WD soils, respectively.

Discussion

Both contemporary conditions and historical soil drainage mediated N_2O and CO_2 emissions from mesic soils in an agricultural field. Large rain events stimulated net N_2O flux in WD soils and inhibited it in PD soils (Fig. 2a, b). Hotspots of N_2O efflux along topographic gradients have previously been attributed to the effect of contemporary soil moisture (Turner et al. 2016). Indeed, large rain events only caused ponding in the PD soils where surface soil O_2 concentrations fell near 0% (Fig. 1b). However, N_2O emissions were not just due to different contemporary ponding status, as ponding treatments in the laboratory experiment stimulated N_2O production via heterotrophic denitrification to a greater degree in WD compared to PD soils (Fig. 5a). Soil CO_2 efflux was also inhibited after large rain events (Fig. 2a, c), but autotrophic respiration may have obscured any patterns between rain events in the field due to the contribution of root respiration to soil respiration during the growing season. Under lab conditions, soil CO_2 efflux was consistently greater from PD soils (Fig. 4b). Ponding initially inhibited CO_2 efflux from both drainage classes, but CO_2 emissions rose as ponding duration increased (Figs. 4b, 5d). These results suggest that soil drainage legacy effects are important regulators of soil GHG emissions. Here, we discuss potential mechanisms driving these effects, and what implications they have for understanding how soil GHG emissions will respond to amplification of the hydrological cycle.

The increased residence time of N_2O under low redox conditions in the PD soils suggests that increased complete denitrification to N_2 could be responsible for the inhibition of net N_2O fluxes in PD soils under ponded conditions (Chapuis-Lardy et al. 2007). However, measurements of gross N_2O production and consumption in the field demonstrated that net N_2O fluxes were due to changes to gross N_2O production rather than N_2O consumption (Fig. 3c, d). The suppression of N_2O production under flooded soil conditions could directly result from the inhibition of the aerobic processes of nitrifier nitrification or nitrifier denitrification which can release N_2O as a byproduct or intermediate product of nitrification, respectively (van Groenigen et al. 2015). Inhibition of nitrifiers under anaerobic conditions can also indirectly decrease net N_2O efflux by limiting the nitrification-derived NO_3^- supply for N_2O production via denitrification. The latter is likely a more important mechanism because a laboratory ^{15}N tracer experiment showed that denitrifiers dominated over nitrifiers as the N_2O source in both soil drainage classes (Fig. 5a, b). The use of loose (albeit unsieved) soil for this experiment may have caused some soil aggregates to disperse, thus releasing labile soil C to fuel denitrification (Schimel et al. 1989), and the even distribution of soil organic matter by soil homogenization for the experiment may have inhibited nitrification by favoring heterotrophs that compete better for NH_4^+ under C-rich conditions (Booth et al. 2006). However, artifacts of soil structure treatment on soil N cycling rates are not always detectable or consistent across studies (Yang et al. 2017). Early in the growing season when soil NO_3^- concentrations are still high from fertilizer application and low plant

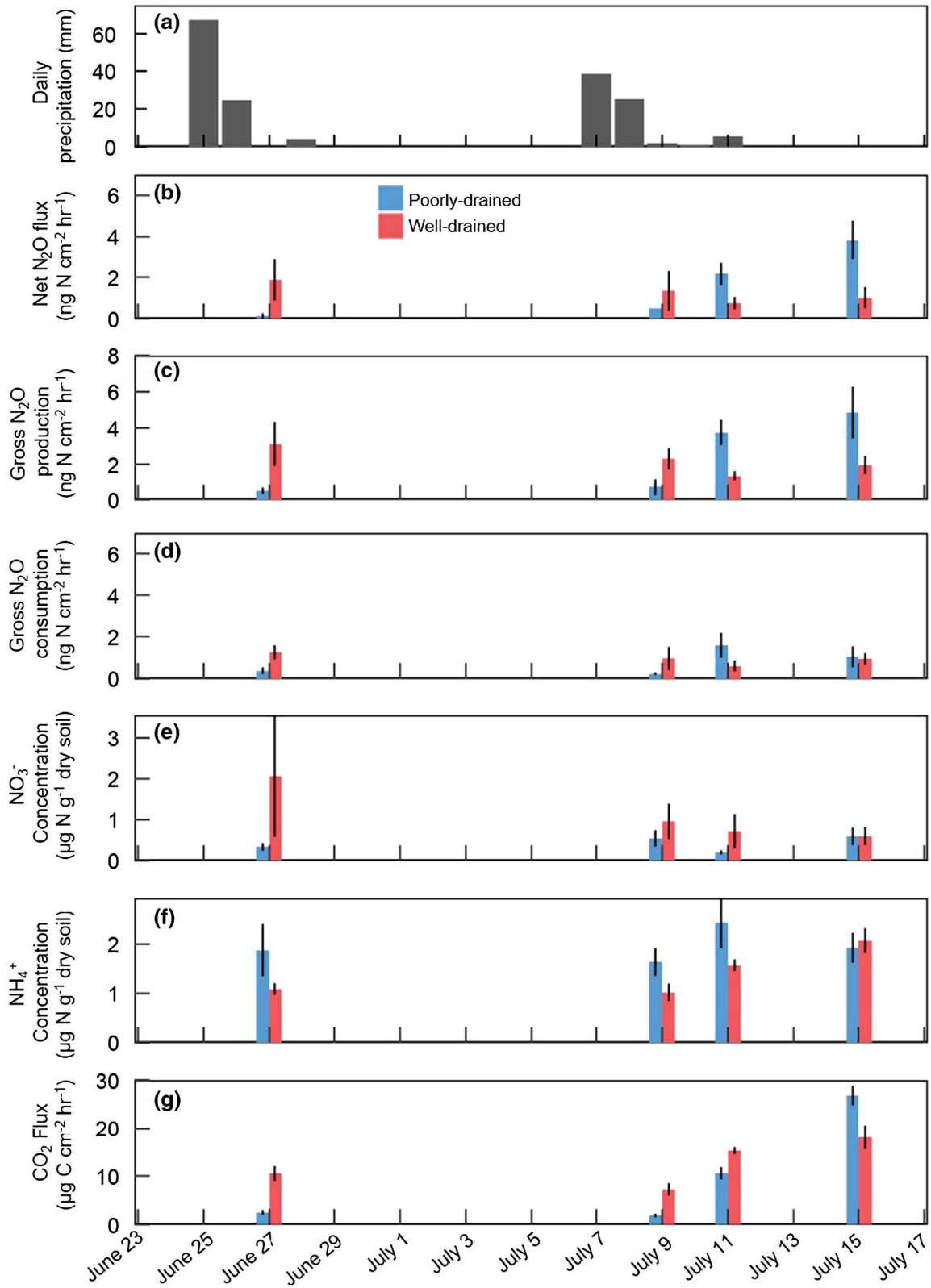
(a)
Daily precipitation (mm)
60
40
20
0
(b)
Poorly-drained
Well-drained
Net N_2O flux (ng N cm^{-2} hr^{-1})
6
4
2
0
(c)
Gross N_2O production (ng N cm^{-2} hr^{-1})
8
6
4
2
0
(d)
Gross N_2O consumption (ng N cm^{-2} hr^{-1})
6
4
2
0
(e)
NO_3^- Concentration (µg N g^{-1} dry soil)
3
2
1
0
(f)
NH_4^+ Concentration (µg N g^{-1} dry soil)
2
1
0
(g)
CO_2 Flux (µg C cm^{-2} hr^{-1})
30
20
10
0
June 23
June 25
June 27
June 29
July 1
July 3
July 5
July 7
July 9
July 11
July 13
July 15
July 17

◀**Fig. 3** Daily precipitation (**a**), net N_2O flux (**b**), gross N_2O production rate (**c**), gross N_2O consumption rate (**d**), NO_3^- concentration (**e**), NH_4^+ concentration (**f**), and CO_2 flux (**g**) measured in the field on 4 days during summer 2015. Error bars represent one standard error (n = 6)

Table 2 N_2O yield from the 2015 field measurements (n = 6)

Date	N_2O yield (mean ± SE)	
	Poorly-drained	Well-drained
June 27*	0.15 ± 0.15^{a}	0.55 ± 0.08^{ab}
July 9*	0.16 ± 0.16^{ab}	0.44 ± 0.20^{ab}
July 11	0.60 ± 0.14^{ab}	0.47 ± 0.17^{ab}
July 15	0.83 ± 0.05^{b}	0.42 ± 0.16^{ab}

Letters indicate significant differences measured by Tukey corrected multiple comparisons ($p < 0.05$). Asterisks indicate dates within 48 h of rainfall

nitrogen demand, depressed areas can serve as N_2O hot spots when ponding creates conditions conducive for denitrification in the presence of ample NO_3^- supply (Molodovskaya et al. 2012; Saha et al. 2017). In contrast, our study took place later in the growing season when soil NO_3^- concentrations were low, thereby limiting denitrification rates in ponded depressed areas to create N_2O cold spots (Turner et al. 2016).

The drainage class differences in in situ gross N_2O production rates following intense rain events cannot be explained solely by contemporary ponding status, as net N_2O efflux differed between soils from the two drainage classes when exposed to the same flooding treatments (Fig. 4a). Well-drained soils supported higher rates of denitrifier-derived N_2O production compared to PD soils under flooded conditions (Fig. 5a), possibly by retaining microsites of high O_2 concentrations within soil macroaggregates (Askaer et al. 2010) that could support coupled nitrification–denitrification under flooded conditions. Although minor soil compaction while collecting soil cores can alter soil pore structure, this pattern observed in the laboratory experiment is consistent with the patterns in N_2O dynamics that we observed in the field. Over time, soil drainage can alter the size class of soil aggregates, which affects the distribution of O_2 throughout the soil profile. Specifically, prolonged anaerobic conditions, as were observed in the PD class, can break down soil macroaggregates (De-Campos et al. 2009). Additionally, plants are more productive in WD compared to PD soils (Grable and Siemer 1968; Kanwar et al. 1988), and plant roots and

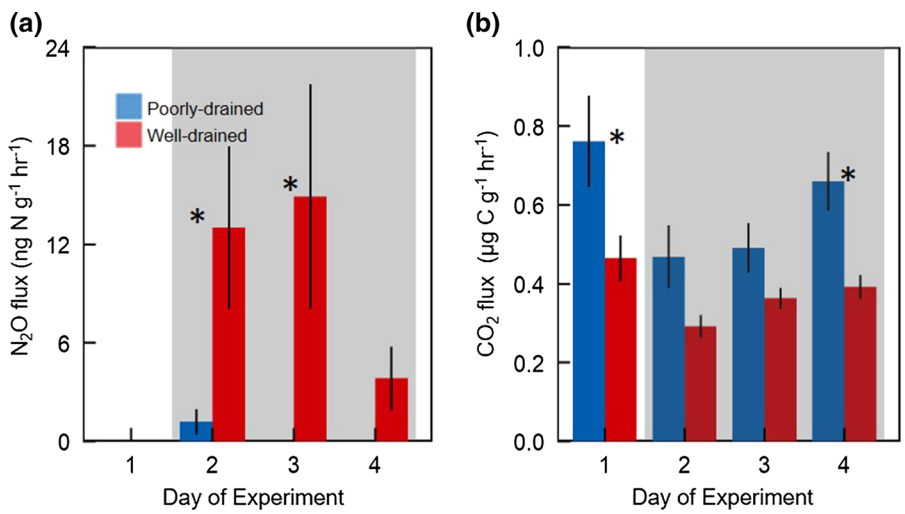

Fig. 4 Net N_2O (**a**) and CO_2 (**b**) flux from the N_2O source experiment in 2015. Error bars represent one standard error (n = 6). The shaded area represents when all the cores were under flooded conditions. On day 1, soils were at field moisture. Asterisks indicate statistically significant differences between PD and WD soils on each day. For day 1, this was determined using a paired t-test. For days 2–4, this was determined using Tukey HSD corrected multiple pairwise comparisons ($p \leq 0.05$). No significant net N_2O fluxes were detected on day 1 from either drainage class, and no significant net N_2O flux was detected from the PD soils on days 3 and 4

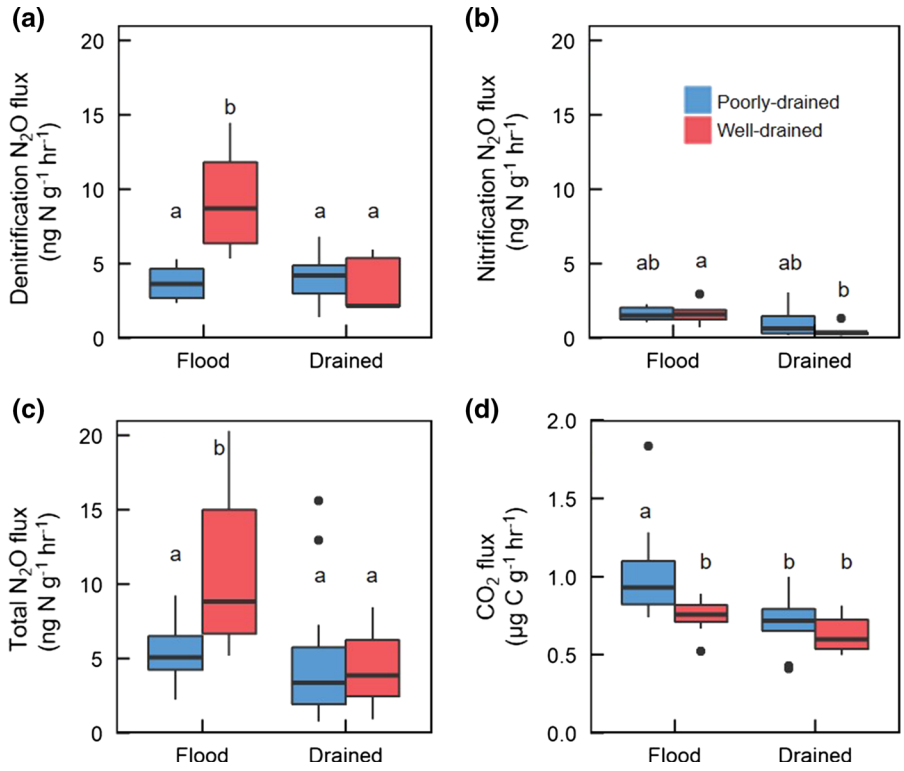

Fig. 5 Denitrification-derived net N_2O flux (**a**) nitrification-derived net N_2O flux (**b**), total net N_2O flux (**c**), and CO_2 flux (**d**) measured on day 5 of the 2015 N_2O source lab experiment. Letters represent significant differences between each mean determined using Tukey HSD corrected multiple pairwise comparisons ($p < 0.05$). The line in each box represents the mean (n = 6 for **a**–**c**, n = 12 for **d**), the upper and lower portions of each box correspond to the 25th and 75th percentiles, the whiskers extend to the upper and lower inter-quartile range, and dots represent outliers

fungal hyphae promote the formation of soil pores and aggregates (Horn and Smucker 2005; Six et al. 2004). Combined, these factors can create more macroaggregates within WD soils that can harbor aerobic microsites under flooded conditions (Gupta and Wang 2006; Askaer et al. 2010) that allow nitrification to occur (Banerjee et al. 2016), thus providing NO_3^- to fuel N_2O production via denitrification. As future increases in the magnitude and frequency of intense precipitation events extends ponding into currently WD soils, these newly ponded areas could, therefore, serve as N_2O hot spots throughout the growing season.

Poorly-drained soils maintained higher net N_2O fluxes than the WD soils during interludes between large rain events (Fig. 2a, b), causing a reversal in the locations of N_2O hot spots and cold spots observed during ponding events. As ponded soils drain, the release of stored N_2O can lead to pulses of N_2O emissions from soil that do not represent concurrent biological production of N_2O (Jarecke et al. 2016). However, the PD soils maintained higher net N_2O efflux even during relatively dry periods, such as 20 June 2014, when no rain had fallen in 10 days (Fig. 2a, b). This suggests that a biotic mechanism may explain higher N_2O efflux during these periods. Soil O_2 concentrations at 10 cm depth experienced a higher magnitude decrease in PD soils compared to WD soils following large rain events, and remained lower compared to WD soils for approximately 1–2 weeks (Fig. 1a, b). For example, after the 90 mm rain event on 25–26 June 2015, 10 cm depth O_2 concentrations fell to 0.3% in the PD soils after 4 days, and didn't rise above 10% for another 3 days. Similar patterns were observed throughout the growing season. Thus, the PD soils potentially retained more anaerobic microsites conducive for denitrification that were intermixed with re-oxygenated pore spaces where nitrification could provide a NO_3^- supply. In contrast, the more porous WD soils were likely more quickly and uniformly oxygenated to limit N_2O production via denitrification. This reversal in N_2O hot spots and cold spots mediated by soil structure differences between drainage classes creates a mechanistic framework to predict when and where hot spots of soil N_2O emissions occur, allowing us to advance beyond the perspective of hot spots as occurring in fixed locations and hot moments as events that occur across the spatial domain (Bernhardt et al. 2017; McClain et al. 2003).

The contribution of autotrophic soil respiration to measured CO_2 fluxes likely obscured patterns in in situ heterotrophic soil respiration. Field sampling in this study occurred only during the peak growing season when roots were well-established. On most sampling dates, soil CO_2 fluxes were greater in the WD class than the PD class (Fig. 2c), but this likely reflected patterns in autotrophic soil respiration associated with higher plant productivity in the WD class (Grable and Siemer 1968; Kanwar et al. 1988). In the plant-free soil incubations in the laboratory, CO_2 fluxes were consistently higher in the PD soils than in the WD soils under these experimental treatments (Fig. 4b). Laboratory incubations are not representative of field conditions and reflect activity only in the soil depth increment sampled (i.e., 0–10 cm depth in this study) while not accounting for physical controls on soil–atmosphere gas fluxes. Nonetheless, this laboratory approach was necessary to disentangle the effects of contemporary ponding from that of historical drainage class in surface soils where C availability and, therefore, microbial activity contributing to GHG fluxes tends to be highest (e.g. Blume et al. 2002; Yang and Silver 2016). Our results suggest that historical soil drainage may affect the response of heterotrophic soil respiration to ponding in the field.

Heterotrophic respiration rates in both the PD and WD classes were inhibited initially by flooding but increased as flooding continued. This phenomenon was recently reported in association with Fe reduction releasing labile C from organo-mineral complexes in mineral soils collected from across a topographic gradient (Huang and Hall 2017). The recovery of heterotrophic respiration rates was more rapid in our study, with CO_2 emissions increasing within 4 days of flooding (Figs. 4b, 5d), compared to weeks in the other study. This suggests that flooding could stimulate heterotrophic respiration in Fe-rich mineral soils on time scales relevant to the short duration of ponding that occurs in the field. Furthermore, differences in potential Fe reduction rates between drainage classes may underlay the higher heterotrophic respiration rates observed in the PD class under both flooded and drained treatments. Redox fluctuations can decrease the crystallinity of Fe(III) oxides (Thompson et al. 2011) such that ponding and drainage cycles in depressions can form more reactive Fe(III) pools that can be more rapidly reduced by microbes. Faster redox fluctuations can also lead to the formation of larger reactive Fe(III) pools that support higher Fe reduction rates (Ginn et al. 2017). While we did not measure rates of Fe reduction, the PD drainage class consistently had a larger pool of reduced Fe(II) compared to the WD class in the field (Fig. 2f). Higher heterotrophic respiration rates in the PD soils under flooding and subsequent drainage could, therefore, reflect the release of labile C from organo-mineral complexes caused directly by Fe reduction (Huang and Hall 2017; Pan et al. 2016) or indirectly by pH changes driven by Fe reduction (Grybos et al. 2009). Our findings contribute to growing evidence that the commonly accepted moisture-respiration relationship, which suggests that C mineralization is inhibited under anaerobic conditions (Linn and Doran 1984), does not hold in periodically flooded mineral soils.

Despite higher heterotrophic respiration rates in the PD class than the WD class, TOC was higher in the PD surface soils (Table 1). This would suggest that PD soils have higher organic C inputs compared to WD soils. However, lower crop productivity in the PD class compared to the WD class should lead to lower TOC inputs from root exudates or from crop residues (Grable and Siemer 1968; Kanwar et al. 1988). Therefore, transport of dissolved or particulate C into PD depressed areas, through hydrological flow or erosion (Nitzsche et al. 2017), must be an important source of TOC. Even if this redistribution of C from the WD class to the PD class contributed to the larger TOC pools in the PD class in comparison to the WD class, higher heterotrophic respiration rates in the PD class are unlikely to deplete the labile TOC pool over long time scales but rather these higher rates can be sustained by these C inputs.

Here, we documented how historical soil drainage mediates the response of GHG fluxes from mesic agricultural soils to contemporary conditions. Soils that have not historically ponded exhibited higher N_2O emissions and lower CO_2 emissions when inundated than soils with a long history of episodic ponding. This suggests that we cannot simply extrapolate our understanding of GHG dynamics in PD areas to areas that will experience increased ponding with climate change driven rainfall intensification. We proposed possible mechanisms related to drainage class differences in soil properties that could underlay this soil drainage legacy effect. Microbial community composition also differs by soil drainage history (Suriyavirun et al. 2019) but the functional importance of this

relative to the role of soil properties differences in driving the legacy effect on GHG fluxes is yet to be determined. Determining these mechanisms could not only elucidate the time scales over which this soil drainage legacy effect develops but would also aid in incorporating historical soil drainage into field and regional scale models to better predict how soil GHG emissions will respond to rainfall intensification and feedback on climate change.

Acknowledgements We would like to thank Jonathan Treffkorn, Lily Zhao, and Nate Lawrence for their assistance in the lab and field. This research was funded by the NSF Dimensions of Biodiversity Grant DEB-1831842 to W.H.Y. and R.S.; and by the Francis M. and Harlie M. Clark Research Support Grant, the Lebus Fund Award, and a summer research award from the University of Illinois at Urbana-Champaign's Program in Ecology, Evolution, and Conservation Biology to A.H.K. A.H.K. was supported by the National Science Foundation Integrative Graduate Education and Research Traineeship Program (NSF IGERT 1069157). We also thank two anonymous reviewers for their many helpful suggestions to greatly improve this manuscript.

Compliance with ethical standards

Conflict of interest None.

References

Adu JK, Oades JM (1978) Physical factors influencing decomposition of organic materials in soil aggregates. Soil Biol Biochem 10:109–115. https://doi.org/10.1016/0038-0717(78)90080-9

Algayer B, Le Bissonnais Y, Darboux F (2014) Short-term dynamics of soil aggregate stability in the field. Soil Sci Soc Am J 78:1168–1176. https://doi.org/10.2136/sssaj2014.01.0009

Ambus P, Christensen S (1994) Measurement of N_2O emission from a fertilized grassland: an analysis of spatial variability. J Geophys Res 99:16549–16555. https://doi.org/10.1029/94JD00267

Askaer L, Elberling B, Glud RN et al (2010) Soil heterogeneity effects on O_2 distribution and CH_4 emissions from wetlands: in situ and mesocosm studies with planar O_2 optodes and membrane inlet mass spectrometry. Soil Biol Biochem 42:2254–2265. https://doi.org/10.1016/j.soilbio.2010.08.026

Averill C, Waring BG, Hawkes CV (2016) Historical precipitation predictably alters the shape and magnitude of microbial functional response to soil moisture. Glob Change Biol 22:1957–1964. https://doi.org/10.1111/gcb.13219

Ball BC, Horgan GW, Clayton H, Parker JP (1997) Spatial variability of nitrous oxide fluxes and controlling soil and topographic properties. J Environ Qual 26:1399–1409. https://doi.org/10.2134/jeq1997.00472425002600050029x

Banerjee S, Helgason B, Wang L et al (2016) Legacy effects of soil moisture on microbial community structure and N_2O emissions. Soil Biol Biochem 95:40–50. https://doi.org/10.1016/j.soilbio.2015.12.004

Bernhardt ES, Blaszczak JR, Ficken CD et al (2017) Control points in ecosystems: moving beyond the hot spot hot moment concept. Ecosystems 20:1–18. https://doi.org/10.1007/s10021-016-0103-y

Blume E, Bischoff M, Reichert JM, Moorman T, Konopka A, Turco RF (2002) Surface and subsurface microbial biomass, community structure and metabolic activity as a function of soil depth and season. Appl Soil Ecol 20:171–181. https://doi.org/10.1016/S0929-1393(02)00025-2

Booth MS, Stark JK, Hart SC (2006) Soil-mixing effects on inorganic nitrogen production and consumption in forest and shrubland soils. Plant Soil 289:5–15. https://doi.org/10.1007/s11104-006-9083-6

Chapuis-Lardy L, Wrage N, Metay A et al (2007) Soils, a sink for N_2O? A review. Glob Change Biol 13:1–17. https://doi.org/10.1111/j.1365-2486.2006.01280.x

DeAngelis KM, Silver WL, Thompson AW, Firestone MK (2010) Microbial communities acclimate to recurring changes in soil redox potential status. Environ Microbiol 12:3137–3149. https://doi.org/10.1111/j.1462-2920.2010.02286.x

De-Campos AB, Mamedov AI, Huang C (2009) Short-term reducing conditions decrease soil aggregation. Soil Sci Soc Am J 73:550–559. https://doi.org/10.2136/sssaj2007.0425

De-Campos AB, Huang CH, Johnston CT (2012) Biogeochemistry of terrestrial soils as influenced by short-term flooding. Biogeochemistry 111:239–252. https://doi.org/10.1007/s10533-011-9639-2

Dubinsky EA, Silver WL, Firestone MK (2010) Tropical forest soil microbial communities couple iron and carbon biogeochemistry. Ecology 91:2604–2612. https://doi.org/10.1890/09-1365.1

Estop-Aragonés C, Knorr KH, Blodau C (2013) Belowground in situ redox dynamics and methanogenesis recovery in a degraded fen during dry–wet cycles and flooding. Biogeosciences 10:421–436. https://doi.org/10.5194/bg-10-421-2013

Evans SE, Wallenstein MD (2012) Soil microbial community response to drying and rewetting stress: does historical precipitation regime matter? Biogeochemistry 109:101–116. https://doi.org/10.1007/s10533-011-9638-3

Evans SE, Wallenstein MD (2014) Climate change alters ecological strategies of soil bacteria. Ecol Lett 17:155–164. https://doi.org/10.1111/ele.12206

Firestone MK, Firestone RB, Tiedje J (1980) Nitrous oxide from soil denitrification: factors controlling its biological production. Science 208:749–751. https://doi.org/10.1111/ele.12206

Fox J, Weisberg S (2011) An R companion to applied regression, 2nd edn. Sage, Thousand Oaks

Ginn B, Meile C, Wilmoth J et al (2017) Rapid iron reduction rates are stimulated by high-amplitude redox fluctuations

in a tropical forest soil. Environ Sci Technol 51:3250–3259. https://doi.org/10.1021/acs.est.6b05709
Gleason K (2008) 2008 Midwestern U.S. floods. NOAA's National Climatic Data Center, Ashville
Grable AR, Siemer EG (1968) Effects of bulk density, aggregate size, and soil water suction on oxygen diffusion, redox potentials, and elongation of corn roots. Soil Sci Soc Am J 32:180–186. https://doi.org/10.2136/sssaj1968.03615995003200020011x
Groffman PM, Tiedje JM (1988) Denitrification hysteresis during wetting and drying cycles in soil. Soil Sci Soc Am J 52:1626–1629. https://doi.org/10.2136/sssaj1988.03615995005200060022x
Groffman PM, Tiedje JM (1991) Relationships between denitrification, CO_2 production and air-filled porosity in soils of different texture and drainage. Soil Biol Biochem 23:299–302. https://doi.org/10.1016/0038-0717(91)90067-T
Grybos M, Davranche M, Gruau G et al (2009) Increasing pH drives organic matter solubilization from wetland soils under reducing conditions. Geoderma 154:13–19. https://doi.org/10.1016/j.geoderma.2009.09.001
Gupta SD, Wang D (2006) Water retention in soil. In: Lal R (ed) Encyclopedia of soil science, 2nd edn. Taylor and Francis, New York, pp 1864–1869
Hawkes CV, Keitt TH (2015) Resilience vs. historical contingency in microbial responses to environmental change. Ecol Lett 18:612–625. https://doi.org/10.1111/ele.12451
Hawkes CV, Waring BG, Rocca JD, Kivlin SN (2017) Historical climate controls soil respiration responses to current soil moisture. Proc Natl Acad Sci USA 114:6322–6327. https://doi.org/10.1073/pnas.1620811114
Herman DJ, Brooks PD, Ashraf M et al (1995) Evaluation of methods for nitrogen-15 analysis of inorganic nitrogen in soil extracts. II. Diffusion methods. Commun Soil Sci Plant Anal 26:1675–1685. https://doi.org/10.1080/00103629509369340
Horn R, Smucker A (2005) Structure formation and its consequences for gas and water transport in unsaturated arable and forest soils. Soil Tillage Res 82:5–14. https://doi.org/10.1016/j.still.2005.01.002
Huang W, Hall SJ (2017) Elevated moisture stimulates carbon loss from mineral soils by releasing protected organic matter. Nat Commun 8:1–10. https://doi.org/10.1038/s41467-017-01998-z
Illinois Climate Network (2017) Water and atmospheric resources monitoring program. Illinois State Water Survey, Champaign
Jarecke KM, Loecke TD, Burgin AJ (2016) Coupled soil oxygen and greenhouse gas dynamics under variable hydrology. Soil Biol Biochem 95:164–172. https://doi.org/10.1016/j.soilbio.2015.12.018
Kanwar RS, Baker JL, Mukhtar S (1988) Excessive soil water effects at various stages of development on the growth and yield of corn. Trans ASAE 31:133–141. https://doi.org/10.13031/2013.30678
Knowles R (1982) Denitrification. Microbiol Rev 46:43–70
Kroon PS, Hensen A, Jonker HJJ et al (2007) Suitability of quantum cascade laser spectroscopy for CH_4 and N_2O eddy covariance flux measurements. Biogeosciences 4:715–728. https://doi.org/10.5194/bg-4-715-2007
Lenth RV (2016) Least-squares means: the R package lsmeans. J Stat Softw 69:1–33
Li X, McCarty GW, Lang M et al (2018) Topographic and physicochemical controls on soil denitrification in prior converted croplands located on the Delmarva Peninsula, USA. Geoderma 309:41–49. https://doi.org/10.1016/j.geoderma.2017.09.003
Linn DM, Doran JW (1984) Effect of water-filled pore space on carbon dioxide and nitrous oxide production in tilled and nontilled soils. Soil Sci Soc Am J 48:1267–1272. https://doi.org/10.2136/sssaj1984.03615995004800060013x
Liptzin D, Silver WL (2009) Effects of carbon additions on iron reduction and phosphorus availability in a humid tropical forest soil. Soil Biol Biochem 41:1696–1702. https://doi.org/10.1016/j.soilbio.2009.05.013
Matson PA, Vitousek PM, Livingston GP, Swanberg NA (1990) Sources of variation in nitrous oxide flux from Amazonian ecosystems. J Geophys Res 95:16789–16798. https://doi.org/10.1029/JD095iD10p16789
Matthias D, Yarger DN, Weinbeck RS (1978) A numberical evaluation of chamber methods for determining gas fluxes. Geophys Res Lett 5:765–768. https://doi.org/10.1029/GL005i009p00765
McClain ME, Boyer EW, Dent CL et al (2003) Biogeochemical hot spots and hot moments at the interface of terrestrial and aquatic ecosystems. Ecosystems 6:301–312. https://doi.org/10.1007/s10021-003-0161-9
Min SK, Zhang X, Zwiers FW, Hegerl GC (2011) Human contribution to more-intense precipitation extremes. Nature 470:378–381. https://doi.org/10.1038/nature09763
Molodovskaya M, Singurindy O, Richards BK et al (2012) Temporal variability of nitrous oxide from fertilized croplands: hot moment analysis. Soil Sci Soc Am J 76:1728–1740. https://doi.org/10.2136/sssaj2012.0039
Nitzsche KN, Kaiser M, Premke K et al (2017) Organic matter distribution and retention along transects from hilltop to kettle hole within an agricultural landscape. Biogeochemistry 136:47–70. https://doi.org/10.1007/s10533-017-0380-3
Palta MM, Ehrenfeld JG, Gimenez D et al (2016) Soil texture and water retention as spatial predictors of denitrification in urban wetlands. Soil Biol Biochem 101:237–250. https://doi.org/10.1016/j.soilbio.2016.06.011
Pan W, Kan J, Inamdar S et al (2016) Dissimilatory microbial iron reduction release DOC (dissolved organic carbon) from carbon-ferrihydrite association. Soil Biol Biochem 103:232–240. https://doi.org/10.1016/j.soilbio.2016.08.026
Parkin TB, Kaspar TC (2006) Nitrous oxide emissions from corn-soybean systems in the Midwest. J Environ Qual 35:1496–1506. https://doi.org/10.2134/jeq2005.0183
Peralta AL, Ludmer S, Kent AD (2013) Hydrologic history influences microbial community composition and nitrogen cycling under experimental drying/wetting treatments. Soil Biol Biochem 66:29–37. https://doi.org/10.1016/j.soilbio.2013.06.019
Pett-Ridge J, Silver WL, Firestone MK (2006) Redox fluctuations frame microbial community impacts on N-cycling rates in a humid tropical forest soil. Biogeochemistry 81:95–110. https://doi.org/10.1007/s10533-006-9032-8

Pinheiro J, DebRoy S, Sarkar D, R Core Team (2017) nlme: linear and nonlinear mixed effects models

R Core Team (2014) R: a language and environment for statistical computing. R Foundation for Statistical Computing, Vienna

Saha D, Rau BM, Kaye JP et al (2017) Landscape control of nitrous oxide emissions during the transition from conservation reserve program to perennial grasses for bioenergy. GCB Bioenergy 9:783–795. https://doi.org/10.1111/gcbb.12395

Schimel JP, Jackson LE, Firestone MK (1989) Spatial and temporal effects on plant microbial competition for inorganic nitrogen in a California annual grassland. Soil Biol Biochem 21:1059–1066. https://doi.org/10.1016/0038-0717(89)90044-8

Sey BK, Manceur AM, Whalen JK et al (2008) Small-scale heterogeneity in carbon dioxide, nitrous oxide and methane production from aggregates of a cultivated sandy-loam soil. Soil Biol Biochem 40:2468–2473. https://doi.org/10.1016/j.soilbio.2008.05.012

Six J, Bossuyt H, Degryze S, Denef K (2004) A history of research on the link between (micro)aggregates, soil biota, and soil organic matter dynamics. Soil Tillage Res 79:7–31. https://doi.org/10.1016/j.still.2004.03.008

Suriyavirun N, Krichels AH, Kent AD, Yang WH (2019) Microtopographic differences in soil properties and microbial community composition at the field scale. Soil Biol Biochem 131:71–80. https://doi.org/10.1016/j.soilbio.2018.12.024

Thompson A, Rancourt DG, Chadwick OA, Chorover J (2011) Iron solid-phase differentiation along a redox gradient in basaltic soils. Geochim Cosmochim Acta 75:119–133. https://doi.org/10.1016/j.gca.2010.10.005

Turner DA, Chen D, Galbally IE et al (2008) Spatial variability of nitrous oxide emissions from an Australian irrigated dairy pasture. Plant Soil 309:77–88. https://doi.org/10.1007/s11104-008-9639-8

Turner PA, Griffis TJ, Mulla DJ et al (2016) A geostatistical approach to identify and mitigate agricultural nitrous oxide emission hotspots. Sci Total Environ 572:442–449. https://doi.org/10.1016/j.scitotenv.2016.08.094

USGCRP (2009) Global climate change impacts in the United States. In: Karl TR, Melillo JM, Peterson TC (eds) United States global change research program. Cambridge University Press, New York

Van Groenigen JW, Huygens D, Boeckx P et al (2015) The soil N cycle: new insights and key challenges. Soil 1:235–256. https://doi.org/10.5194/soil-1-235-2015

Villarini G, Smith JA, Vecchi GA (2013) Changing frequency of heavy rainfall over the central United States. J Clim 26:351–357. https://doi.org/10.1175/JCLI-D-12-00043.1

von Fischer JC, Hedin LO (2007) Controls on soil methane fluxes: tests of biophysical mechanisms using table isotope tracers. Glob Biogeochem Cycles 21:1–9. https://doi.org/10.1029/2006GB002687

Wang B, Lerdau M, He Y (2017) Widespread production of nonmicrobial greenhouse gases in soils. Glob Change Biol 23:4472–4482. https://doi.org/10.1111/gcb.13753

Yanai J, Sawamoto T, Oe T et al (1965) Spatial variability of nitrous oxide emissions and their soil-related determining factors in an agricultural field. J Environ Qual 32:1965–1977. https://doi.org/10.2134/jeq2003.1965

Yang WH, Silver WL (2016) Gross nitrous oxide production drives net nitrous oxide fluxes across a salt marsh landscape. Glob Change Biol 22:2228–2237. https://doi.org/10.1111/gcb.13203

Yang WH, Teh YA, Silver WL (2011) A test of a field-based ^{15}N-nitrous oxide pool dilution technique to measure gross N_2O production in soil. Glob Change Biol 17:3577–3588. https://doi.org/10.1111/j.1365-2486.2011.02481.x

Yang WH, Ryals RA, Cusack DF, Silver WL (2017) Cross-biome assessment of gross soil nitrogen cycling in California ecosystems. Soil Biol Biochem 107:144–155. https://doi.org/10.1016/j.soilbio.2017.01.004

Zeglin LHZ, Ottomley PJB, Umpponen AJ et al (2013) Altered precipitation regime affects the function and composition of soil microbial communities on multiple time scales. Ecology 94:2334–2345. https://doi.org/10.1890/12-2018.1